ADVANCED SCIENCE
Open Access

# Supporting Information

for *Adv. Sci.*, DOI: 10.1002/advs.201600122

# Engineering Intrinsically Zirconium-89 Radiolabeled Self-Destructing Mesoporous Silica Nanostructures for In Vivo Biodistribution and Tumor Targeting Studies

*Shreya Goel, Feng Chen, Shijie Luan, Hector F. Valdovinos, Sixiang Shi, Stephen A. Graves, Fanrong Ai, Todd E. Barnhart, Charles P. Theuer, and Weibo Cai**

# Supporting Information

## Engineering Intrinsically Zirconium-89 Radiolabeled Self-Destructing Mesoporous Silica Nanostructures for In Vivo Biodistribution and Tumor Targeting Studies

*Shreya Goel, Feng Chen, Shijie Luan, Hector F. Valdovinos, Sixiang Shi, Stephen A. Graves, Fanrong Ai, Todd E. Barnhart, Charles P.Theuer, Weibo Cai**

S. Goel and S. Shi
Materials Science Program, University of Wisconsin – Madison, Wisconsin 53705

Dr. F. Chen and Dr. F. Ai
Department of Radiology, University of Wisconsin – Madison, Wisconsin 53705

S. Luan
School of Pharmacy, Temple University, Philadelphia, Pennsylvania 19140

H.F. Valdovinos, S. Graves and Dr. T.E. Barnhart
Department of Medical Physics, University of Wisconsin – Madison

Dr. C.P. Theuer
TRACON Pharmaceuticals Inc., San Diego, California 92122

Prof. W. Cai
Materials Science Program, University of Wisconsin – Madison, Wisconsin 53705
Department of Radiology, University of Wisconsin – Madison, Wisconsin 53705
Department of Medical Physics, University of Wisconsin – Madison
University of Wisconsin Carbone Cancer Centre, Madison, Wisconsin 53705
Fax: (+1) 608-265-0614
Email: WCai@uwhealth.org
Homepage: http://mi.wisc.edu

**Keywords:** Biodegradable mesoporous silica nanoparticles, Intrinsic radiolabeling, Positron emission tomography (PET) imaging, Vasculature targeting

**S.1. Theoretical Calculations for the number of nanoparticles (bMSNs)**

Theoretical calculations to determine the number of nanoparticles per gram were based on a previously reported procedure.[1]

Volume of a mesoporous nanoparticle, such as bMSN can be divided into (i) pore volume, ($V_p$) and solid volume ($V_s$). $V_p$ was determined from the BET data, while Vs was determined using the following equation: $Vs = \frac{M_s}{\rho_s} = \frac{1}{2.2} = 0.455\ cm^3$ where Ms is the mass of bMSNs in grams and ρ is the density of silica (2.2 $gcm^{-3}$).

Number of bMSNs per gram $N_{bMSN} = \frac{1}{M_{bMSN}}$, where $M_{bMSN}$ is the mass of each nanoparticle.

$M_{bMSN} = \rho * V_{bMSN} = \rho * \frac{4\pi r^3}{3}(1-\chi)$; where r = radius of bMSN as determined from TEM images (*Figure S2c*; r = 82.68 nm) and χ is the pore volume fraction defined as $\chi = \frac{Vp}{Vp+Vs}$. Therefore, making the appropriate substitutions, number of bMSNs per gram can be estimated to be:

$$N_{bMSN} = \frac{1}{\rho * \frac{4\pi r^3}{3}(1-\frac{Vp}{Vp+Vs})} = \frac{0.749\ (Vp+0.455)}{\pi r^3} = \frac{0.238\ (1.844+0.455)}{(82.68\times10^{-7})^3} = \mathbf{9.68 \times 10^{14}}$$

The theoretically calculated number was found to be very close to that determined using the NanoSight Technology ~**$8.97 \times 10^{11}$ bMSNs $mL^{-1}$** or **$3.59\times 10^{14}$ $g^{-1}$**.

**S.2. Calculation of the number of silanol groups per bMSN**

According to the Zhuravlev model, the number of silanol groups (Si-OH) per unit surface area of amorphous silica is depicted by a physico-chemical constant (known as the Kiselev–Zhuravlev constant) with a numerical value ~4.9 $nm^{-2}$.[2] The number of silanol groups for bMSN (5 v/v%), thus calculated is presented in *Table S1*.

**S.3. Calculation of the number of targeting ligands (TRC105) per bMSN**

Prior to conjugation, TRC105 was derivatized with Traut's Reagent, such that each antibody molecule possessed ~3 –SH moieties (as determined by the Ellman's Reagent test).[3] Initial amount of TRC105-SH added to the nanoparticle solution = 45.80 µg or $1.83 \times 10^{14}$ molecules. After incubation with bMSN-$PEG_{5k}$-Mal (~$8.97 \times 10^{11}$ $mL^{-1}$) for 3 h, the solution was centrifuged at 5000g to remove any unconjugated antibody. Amount of unreacted TRC105-SH in the supernatant was calculated from the Bradford Assay using the standard curve after polynomial fitting (*Figure S4*). Amount of unreacted TRC105-SH was determined to be ~35.82 µg. Thus, ~$4.02 \times 10^{13}$ molecules of TRC105-SH were finally conjugated to the bMSN-$PEG_{5k}$-Mal. Considering the number of nanoparticles per reaction to be ~$8.97 \times 10^{11}$ $mL^{-1}$, the number of TRC105-SH conjugated per nanoparticle per mL was determined to be **~44.6**.

**S.4. Prediction of elimination half-life ($t_{1/2\beta}$) of [$^{89}$Zr]bMSN-$PEG_{5k}$-TRC105**

Elimination half-life ($t_{1/2\beta}$) of [$^{89}$Zr]bMSN-$PEG_{5k}$-TRC105 was roughly estimated using the quantification data obtained from serial PET scans in 4T1 tumor bearing mice (n = 4). Equal volume regions-of-interest (ROIs) were drawn over the heart tissue in the PET images and used to calculate percentage injected dose per gram of tissue (%ID/g) at each time-point. All data was decay corrected and processed as previously described.[4] Bi-exponential fitting of the time-activity curve was used to estimate $t_{1/2\beta}$ of [$^{89}$Zr]bMSN-$PEG_{5k}$-TRC105 (*Figure S7*).

**SUPPLEMENTARY TABLES AND FIGURES**

**Table S1.** Number of silanol groups per nanoparticle

| | **Radius (nm)** | **Surface Area ($m^2$/g)** | **No. of Nanoparticles per gram** | **Surface Area per Nanoparticle ($nm^2$)** | **Total Number of Silanol Groups per Nanoparticle** |
|---|---|---|---|---|---|
| **bMSN(5 v/v%)** | 82.68 | 741.92 | $3.59\times 10^{14}$ | $2.06\times 10^{6}$ | $1.01\times 10^{7}$ |

**Table S2.** Sunitinib (SUN) loading and release

| | **Amount Loaded (mg)** | **Loading Capacity (mg/g)** | **Loading Efficiency (%)** | **Cumulative Release (%)** |
|---|---|---|---|---|
| **dSN** | 0.17 | 46.63 | 8.39 | - |
| **MSN** | 0.56 | 155.09 | 27.9 | 56.41 |
| **bMSN** | 0.83 | 295.95 | 41.4 | 68.90 |

**Table S3.** Bovine Serum Albumin (BSA) loading and release

| | **Amount Loaded (mg)** | **Loading Capacity (mg/g)** | **Loading Efficiency (%)** | **Cumulative Release (%)** |
|---|---|---|---|---|
| **dSN** | 0.02 | 20.00 | 1.5 | - |
| **MSN** | 0.15 | 250.00 | 15.0 | 80.0 |
| **bMSN** | 0.33 | 589.28 | 32.5 | 90.77 |

**Table S4.** Temporal variation in labeling yields of bMSN-$NH_2$ in 0.1 M HEPES buffer at 75 °C under different pH conditions

| | **pH 2** | **pH 7** |
|---|---|---|
| **30 min** | 19.1 | 67.2 |
| **60 min** | 28.1 | 88.5 |
| **120 min** | 30.7 | 94.7 |

**Table S5.** Change in zeta potential during the stepwise synthesis of [$^{89}$Zr]bMSN-$PEG_{5k}$-TRC105. All measurements were performed in PBS (pH 7.4)

| | **Zeta Potential (mV)** |
|---|---|
| **bMSN** | -48.37 ± 0.31 |
| **bMSN-$NH_2$** | 9.58 ± 0.92 |
| **bMSN-$PEG_{5k}$** | -2.78 ± 0.33 |
| **bMSN-$PEG_{5k}$-TRC105** | -1.28 ± 0.39 |
| **[$^{89}$Zr]bMSN-$PEG_{5k}$-TRC105** | -0.16 ± 0.06 |

**Table S6.** Tumor-to-muscle ratios calculated based on the PET ROI values (n=3)

| | **Targeted** | **Non-targeted** | **Blocking** |
|---|---|---|---|
| **0.5 h** | 7.49 ± 2.55 | 2.16 ± 0.68 | 3.39 ± 0.64 |
| **4 h** | 25.89 ± 3.55 | 5.04 ± 0.85 | 5.74 ± 0.17 |
| **24 h** | 47.18 ± 7.19 | 9.75 ± 2.07 | 9.92 ± 2.82 |
| **48 h** | 47.19 ± 8.41 | 7.95 ± 1.64 | 8.84 ± 2.32 |

**Table S7.** Simulated Body Fluid (SBF) composition (pH 7.4; 1 L)

| **Reagent** | **Amount** |
|---|---|
| NaCl | 7.996 g |
| $NaHCO_3$ | 0.350 g |
| KCl | 0.224 g |
| $K_2HPO_4 \cdot 3H_2O$ | 0.228 g |
| $MgCl_2 \cdot 6H_2O$ | 0.305 g |
| 1M-HCl | 40 mL |
| $CaCl_2$ | 0.278 g |
| $Na_2SO_4$ | 0.071 g |
| $(CH_2OH)_3CNH_2$ | 6.057 g |

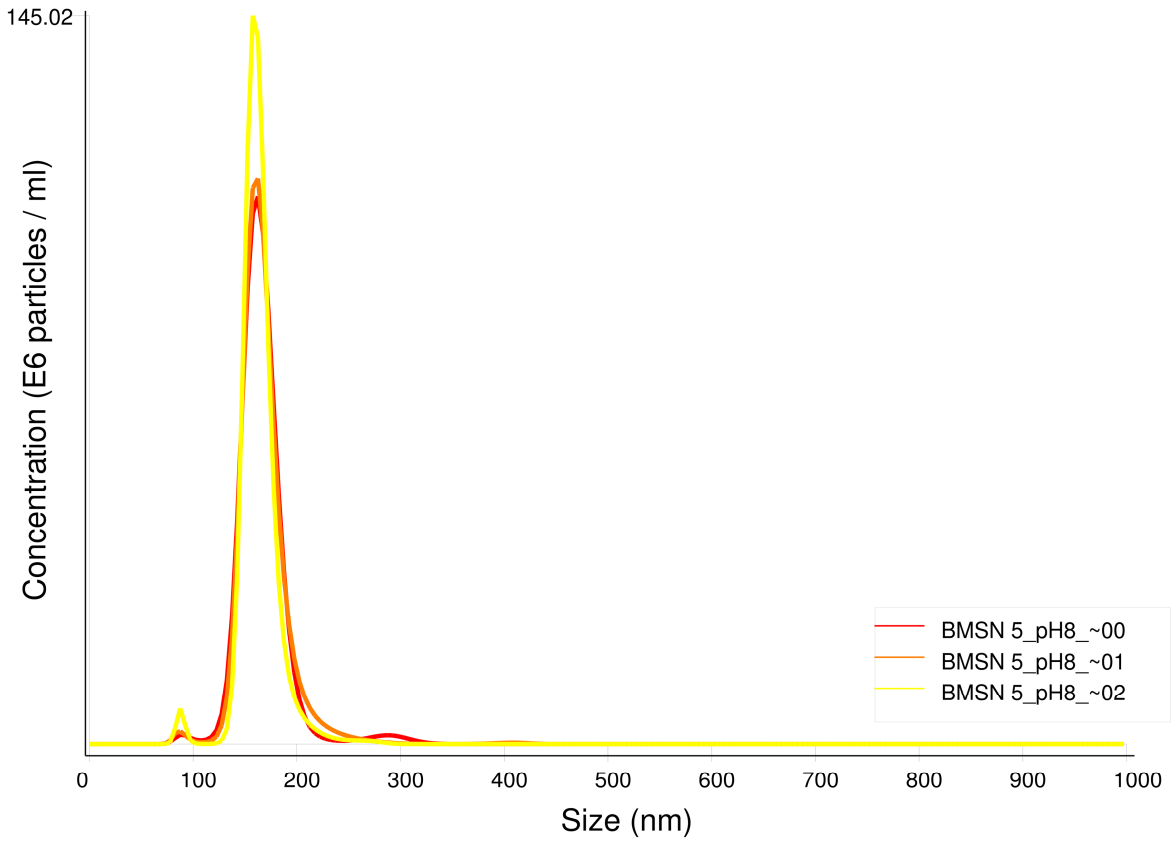


**Figure S1.** Size-Concentration graph for 1000-times diluted solution of bMSN (5 v/v%).

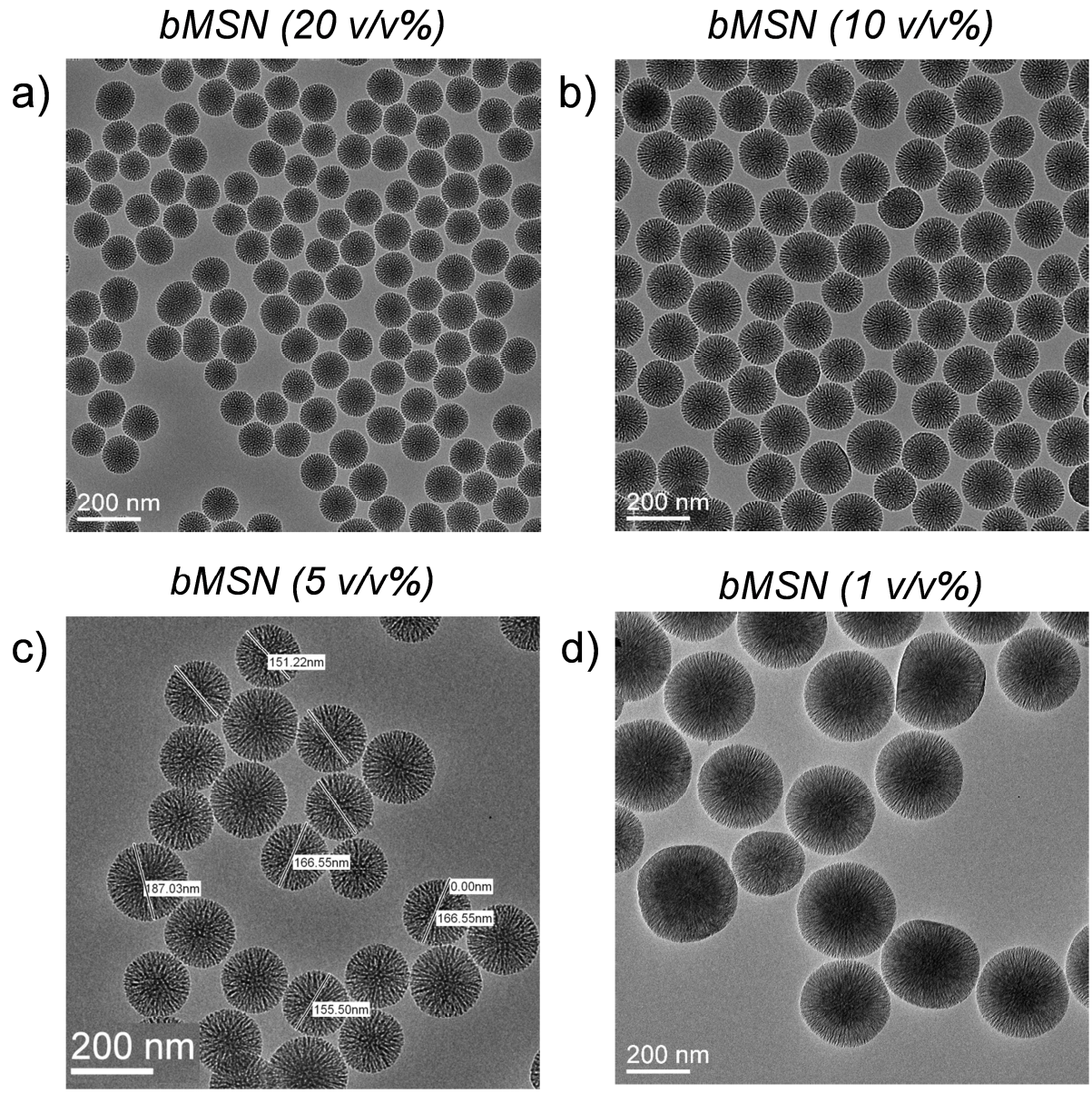


**Figure S2.** TEM images of bMSNs with varying compositions (TEOS: cyclohexane ratios) and pore sizes. (a) 20 v/v % (b) 10 v/v %, (c) 5 v/v % and (d) 1 v/v%

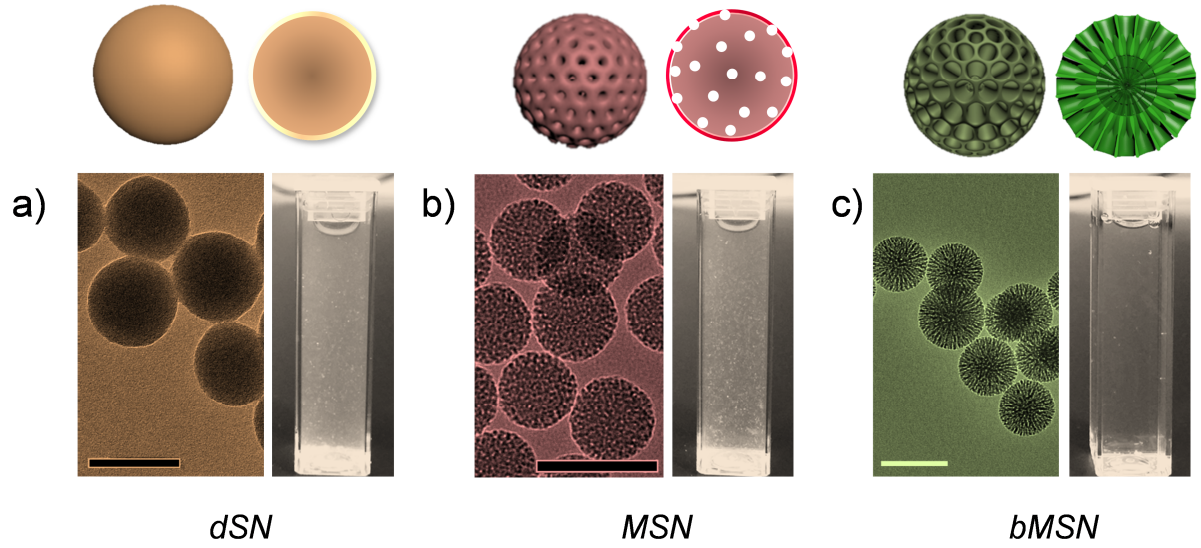


**Figure S3.** (**a**) TEM image of dSN (left) and a photograph of dSN solution after 21 days of incubation in SBF. (**b**) TEM image of MSN (left) and a photograph of MSN solution after 21 days of incubation in SBF. (**c**) TEM image of bMSN (left) and a photograph of bMSN solution after 21 days of incubation in SBF. Schematic on the top depicts the 3-D morphology and 2-D cross-sections of the corresponding nanoparticles.

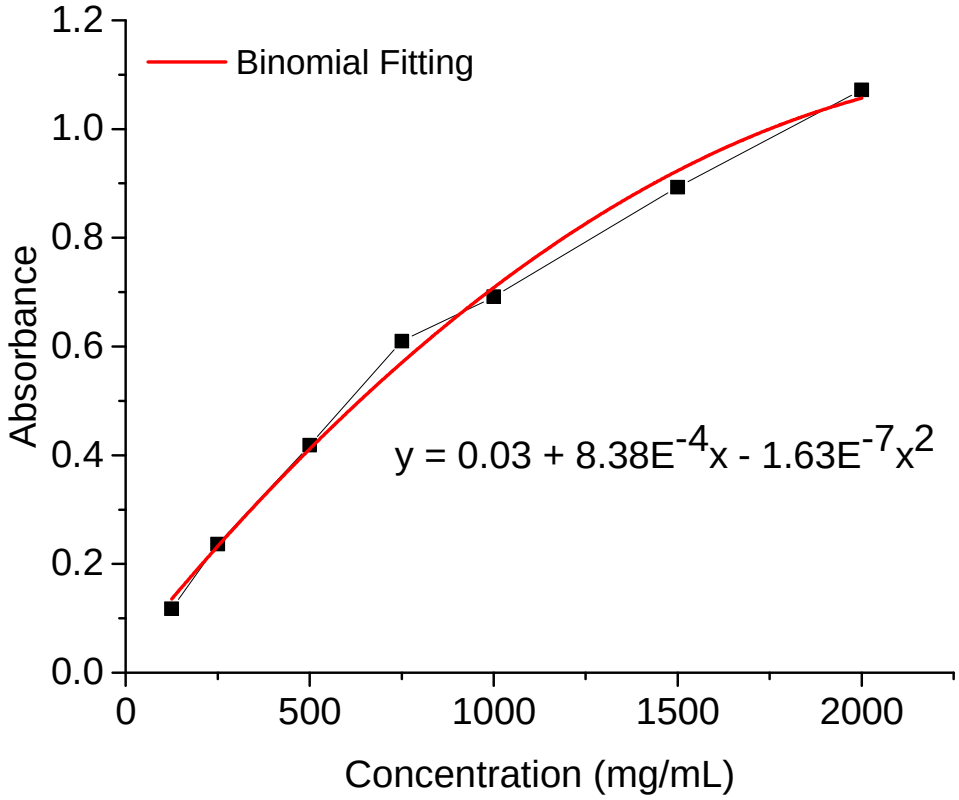


**Figure S4.** Equation and standard curve from Bradford Assay for calculation of number of TRC105 per bMSN.

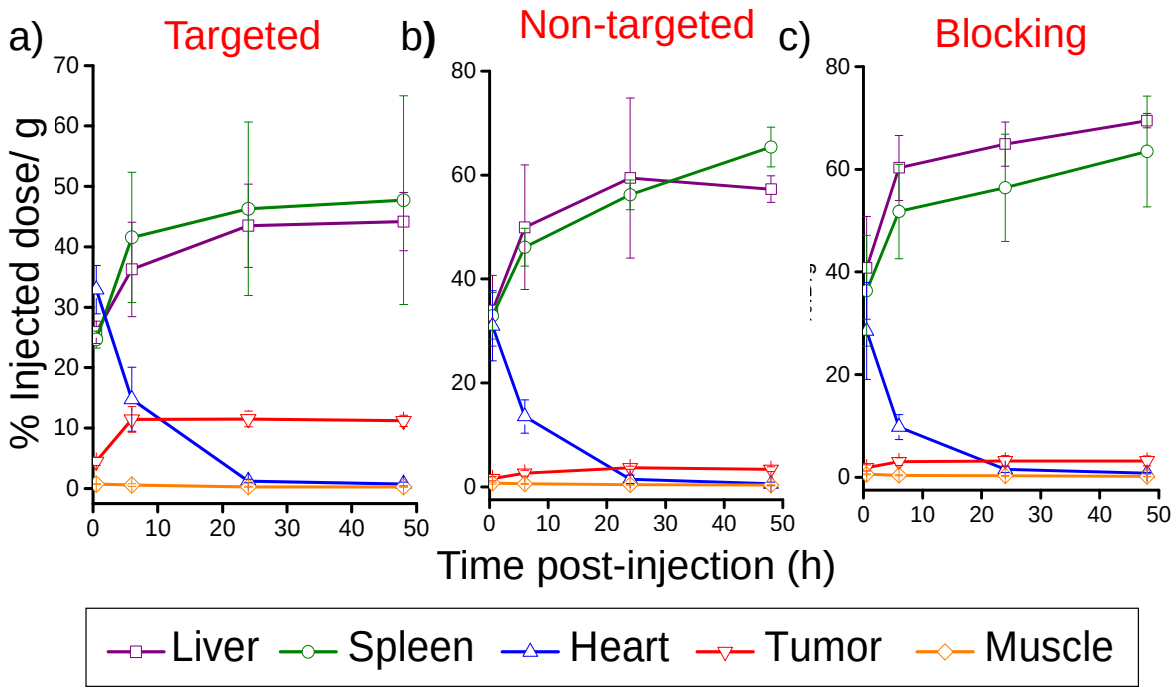


**Figure S5.** Region-of-interest (ROI) quantification. Time-activity curves for (**a**) targeted, (**b**) non-targeted, and (**c**) blocking groups.

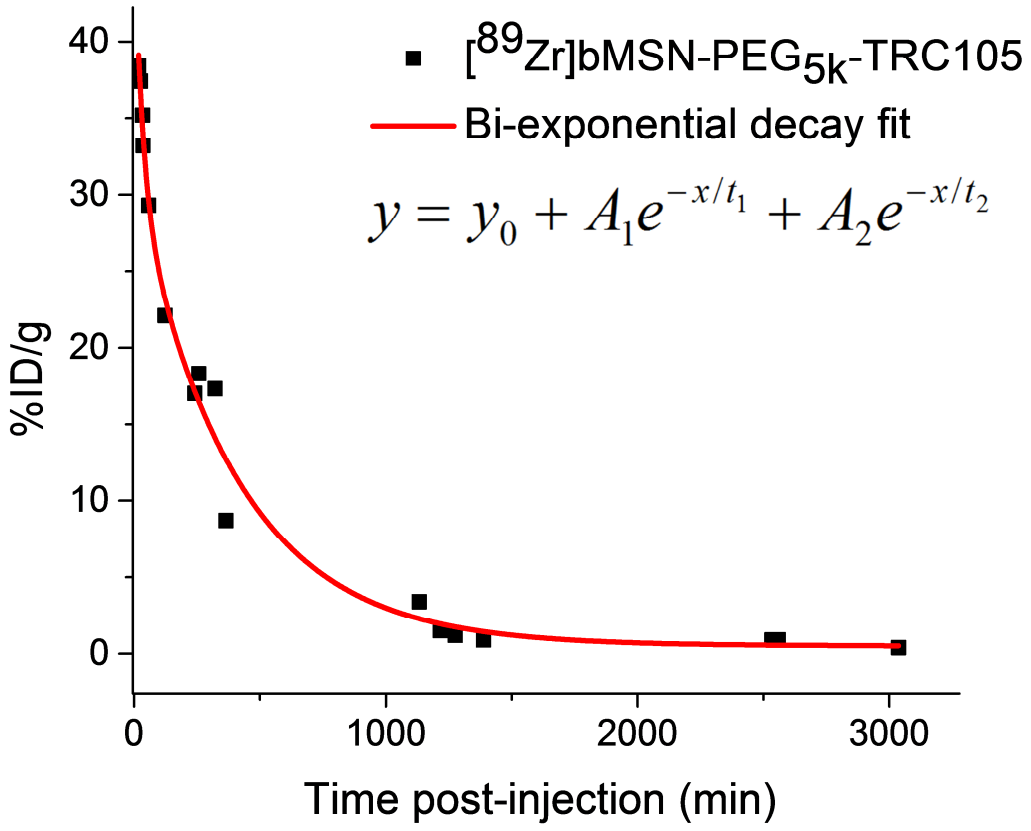


**Figure S6.** Bi-exponential fitting of the time-activity curve to determine the elimination half-life ($t_{1/2\beta}$) for [$^{89}$Zr]bMSN-PEG$_{5k}$-TRC105.

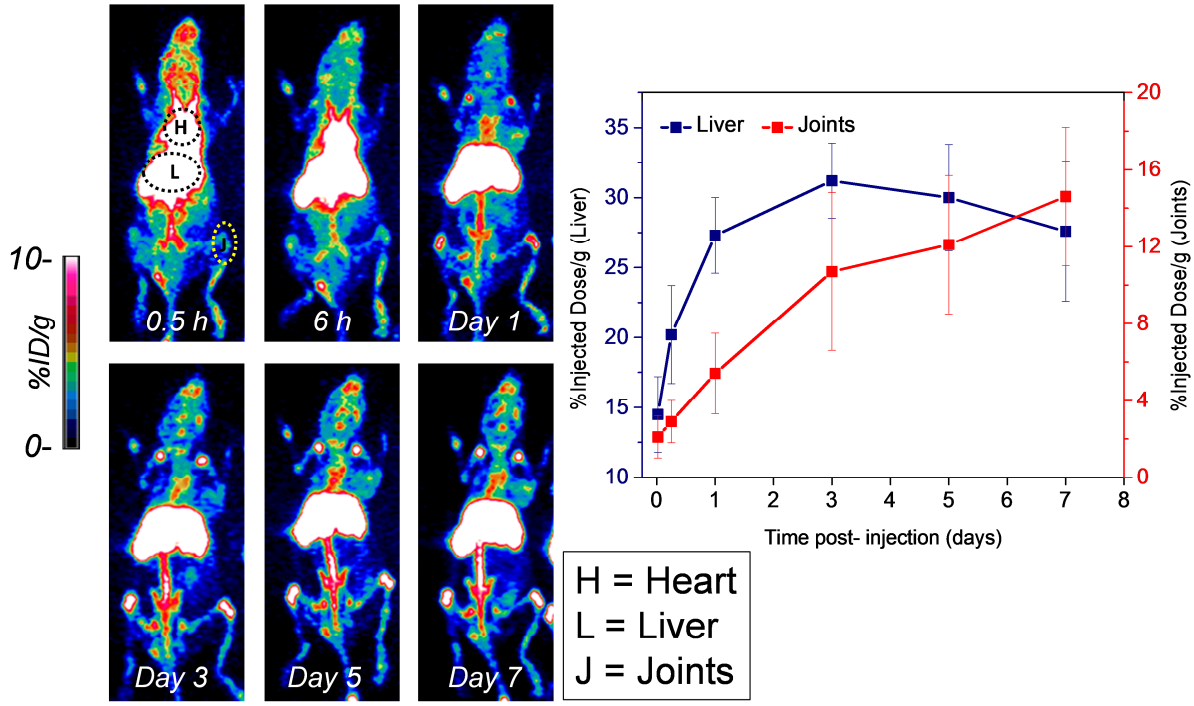


**Figure S7.** (**a**) Maximum-intensity-projections (MIP) of long term fate of [$^{89}$Zr]bMSN-PEG$_{5k}$-TRC105 in healthy mice.

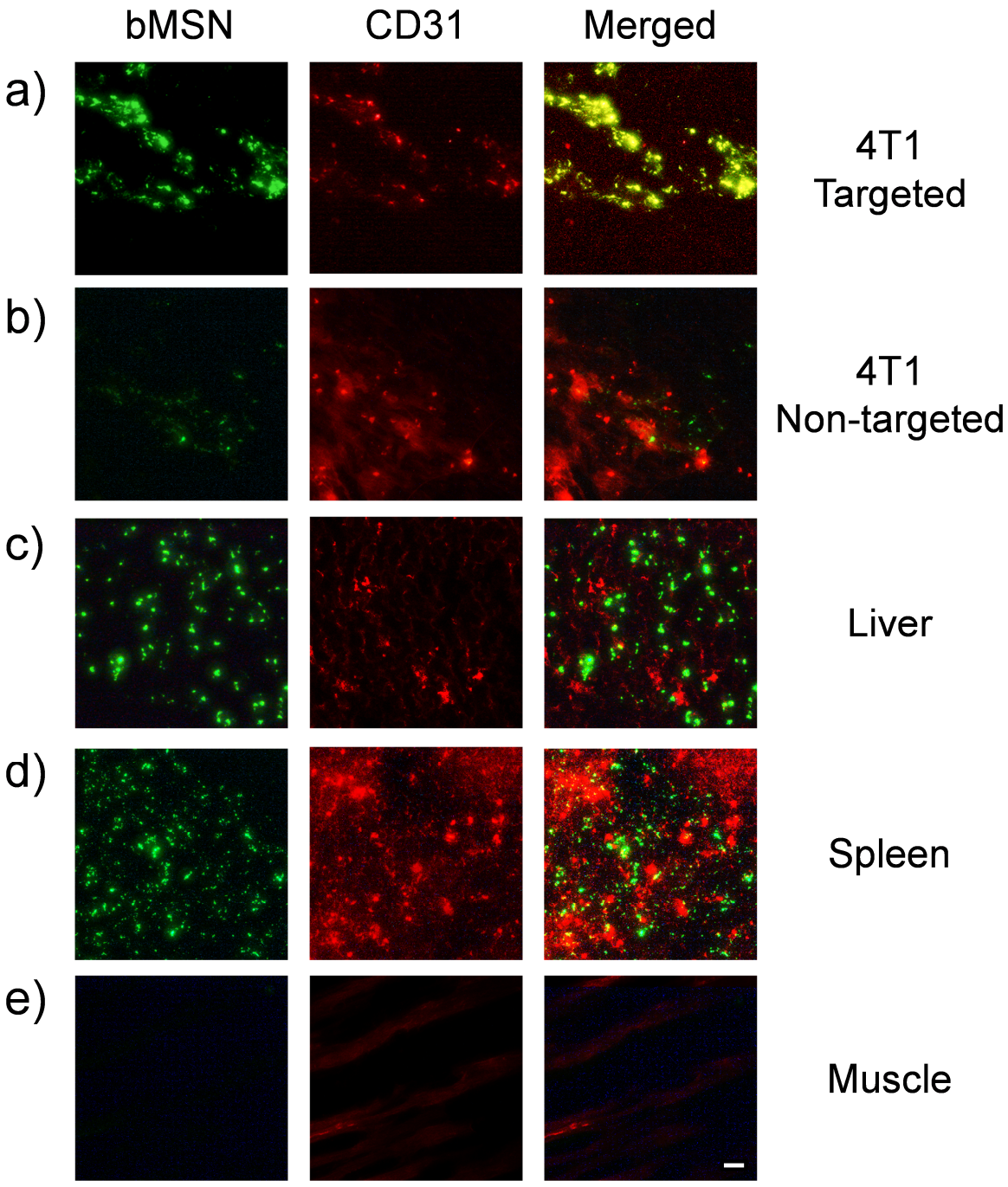


**Figure S8.** Ex vivo histology 6 h p.i. Fluorescein conjugated bMSNs are shown in green, (left panel) and immuno-stained CD31 is shown in red (middle panel). Merged images are also shown. Scale bar presents 50 µm.

**References**

[1] L. Pan, Q. He, J. Liu, Y. Chen, M. Ma, L. Zhang, J. Shi, *J Am Chem Soc* 2012, 134, 5722.

[2] Y. S. Lin, C. L. Haynes, *J Am Chem Soc* 2010, 132, 4834.

[3] L. T. Zhuravlev, *Colloids Surf A* 2000, 173, 1.

[4] J. Woodward, J. Tate, P. C. Herrmann, B. R. Evans, *J Biochem Biophys Methods* 1993, 26, 121.

[5] H. Hong, G. W. Severin, Y. Yang, J. W. Engle, Y. Zhang, T. E. Barnhart, G. Liu, B. R. Leigh, R. J. Nickles, W. Cai, *Eur J Nuc Med Mol Imaging* 2012, 39, 138.